

---

<https://doi.org/10.15407/ujpe71.2.188>

L. KALANDADZE, O. NAKASHIDZE, N. GOMIDZE,  
M. KHAJISHVILI, I. JABNIDZE, K. MAKHARADZE

Department of Physics, Batumi Shota Rustaveli State University  
(*Batumi 6010, Georgia*)

## MAGNETO-OPTICAL BEHAVIOR OF IMPLANTED FERRITE-GARNET THIN FILMS IN THE TRANSPARENCY RANGE<sup>1</sup>

---

*Ferrite-garnet thin films exhibit peculiar magneto-optical properties, which make them highly relevant for both fundamental research and advanced technological applications in optics, magnetism, electronics, spintronics, and photonics. From this perspective, particular practical importance is attributed to the magneto-optical properties of ion-implanted ferrite-garnet films, as ion implantation can reduce or modify local magnetization, coercivity, and anisotropy, as well as weaken cylindrical magnetic domains, thereby enhancing the control and utilization of their parameters. In the present paper, we investigate the magneto-optical Kerr effect in the range of incident light quantum energy of 0.5–4.5 eV before and after ion-implantation of ferrite-garnet films for different compositions  $(YBiCaSmLu)_3(FeGeSi)_5O_{12}$ ,  $(YBiCa)_3(FeGe)_5O_{12}$ , and  $(YBiCaSm)_3(FeGeSi)_5O_{12}$ . It has been established that ferrite-granite thin films exhibit interesting magneto-optical properties in the range of incident light quantum energy of 0.5–2.2 eV. In particular, under certain experimental conditions, magneto-optical activity is observed when the plane of polarization of the incident light deviates from the P-component. To clarify the nature of this effect, the polar Kerr effect and magnetization processes in the energy range of incident light quanta of 0.5–2.2 eV, which is the transparency region of ferrite-garnet, were studied. The obtained results confirm that in this region, magneto-optical activity is characteristic of all three compositions of ferrite-garnet, and implantation has virtually no effect on their magneto-optical properties.*

*Keywords:* ferrite-garnet thin films, soft magnetic materials, ion implantation, magneto-optical materials, magneto-optical effects.

### 1. Introduction

Ferrite-garnet thin films are among the most prominent magneto-optical materials due to their combi-

---

Citation: Kalandadze L., Nakashidze O., Gomidze N., Khashishvili M., Jabinidze I., Makharadze K. Magneto-optical behavior of implanted ferrite-garnet thin films in the transparency range. *Ukr. J. Phys.* **71**, No. 2, 188 (2026). <https://doi.org/10.15407/ujpe71.2.188>.

© Publisher PH “Akademperiodyka” of the NAS of Ukraine, 2026. This is an open access article under the CC BY-NC-ND license (<https://creativecommons.org/licenses/by-nc-nd/4.0/>)

nation of large Faraday rotation, strong Kerr effect, and a wide optical transparency window spanning the visible and near-infrared spectral ranges [1–5]. Bismuth-substituted garnets achieve some of the highest magneto-optical activity, enabling their widespread use in optical isolators, circulators, and integrated photonic devices. Their domain structures provide direct visualization of magnetic patterns, making them useful for magneto-optical imaging and fundamen-

---

<sup>1</sup> This work is based on the results presented at the 2025 “New Trends in High-Energy Physics” Conference.

tal studies of micromagnetism [5–7]. Historically applied in data storage, ferrite-garnet films have now become essential for advanced photonics, spintronics, and magnetophotonics, with ongoing research focusing on nanoscale engineering and integration for next-generation communication and quantum information systems [8, 9].

Ion implantation is widely used both as a tool to modify their magneto-optical and magnetic properties locally and as a fabrication technique for integrated magneto-optical devices. Implantation can reduce or alter local magnetization, coercivity, and anisotropy, as well as weaken domain pinning, which allows for the creation of patterned magnetic regions [10–12]. Heterogeneous magnetic structures can form in the surface layer of a ferrite-garnet films due to ion implantation [13, 14].

The development and utilization of implanted ferrite-garnet thin films rely on studying and controlling their magnetic, optical, and magneto-optical properties. In this context, magneto-optical research methods are crucial for examining their magneto-optical behaviors [15, 16]. The study of samples using magneto-optical methods offers several advantages, including simplicity, minimal impact on the sample structure, and the ability to gather extensive information from measurements. For instance, spectral measurements of the equatorial Kerr effect can reveal details about a sample's microstructure, spin transitions, anisotropy, and magnetic phase changes. Moreover, comparing spectral curves with each other allows a visual comparison of samples and enables one to obtain information about the influence of certain substances on the compositional structure of the sample, both across the entire spectrum and in its specific spectral regions [9, 10, 17–19]. For this reason, a comprehensive study of the magneto-optical properties of nanoheterostructures, thin films, implanted surfaces, and other ultrafine structures – taking into consideration their structural composition and fabrication technology – is significant for understanding the fundamental principles governing the formation of their physical properties.

In the present paper, we investigate the magneto-optical Kerr effect in the range of incident light quantum energy of 0.5–4.5 eV before and after ion-implantation of ferrite-garnet films for different compositions  $(\text{YBiCaSmLu})_3(\text{FeGeSi})_5\text{O}_{12}$ ,  $(\text{YBiCa})_3(\text{FeGe})_5\text{O}_{12}$ , and  $(\text{YBiCaSm})_3(\text{FeGeSi})_5\text{O}_{12}$ .

During our experimental exploration of the samples, we focused on the transparent region of the ferrite-garnet thin films, which range from 0.5 to 2.2 eV. Typically, in this spectral range, magneto-optical reflection effects are almost nonexistent. However, in our case, we observed measurable magneto-optical activity in both implanted and non-implanted ferrite-garnet thin films within this region. We conducted further research with a specific focus on this range. The magneto-optical properties were measured using two different Kerr configurations: polar and transverse. We examined how ion implantation affects the rotation of the polarization plane and the intensity of reflected light based on the orientation of the incident light's polarization plane. Additionally, we explored its impact on the magnetization processes in the transparency region of garnet films, aiming to understand the nature of these effects.

The investigation of the magneto-optical properties of ferrite-garnet films in the transparency range is essential due to their potential applications in spintronics and photonics, highlighting the need for further research [19–21].

## 2. Experimental Details

In our experiments, we utilized  $(\text{YBiCaSmLu})_3(\text{FeGeSi})_5\text{O}_{12}$ ,  $(\text{YBiCa})_3(\text{FeGe})_5\text{O}_{12}$ , and  $(\text{YBiCaSm})_3(\text{FeGeSi})_5\text{O}_{12}$  garnet films with thicknesses of 2.2, 1.0, and 1.3 micrometers ( $\mu\text{m}$ ), respectively, exhibiting uniaxial perpendicular magnetic anisotropy. These films were prepared using liquid-phase epitaxy on  $\text{Gd}_3\text{Ga}_5\text{O}_{12}$  substrates with a thickness of 450  $\mu\text{m}$  and (111) crystallographic orientation. The implantation process was carried out at room temperature using  $\text{Ne}^+$  ions with an energy of 100 keV and varying doses ranging from  $0.5 \times 10^{14}$  to  $2.5 \times 10^{14}$  ions/ $\text{cm}^2$ . During this process, the penetration depth of the implanted ions was 0.1  $\mu\text{m}$ , with the highest concentration of implanted ions located at a depth of 0.07  $\mu\text{m}$ .

The schematic of the experimental setup for measuring magneto-optical reflection effects is illustrated in Fig. 1.

To define magneto-optical properties, a dynamic method was employed. Light transmitted through the optical system—comprising an L-lens, P-polarizer, DMR-monochromator, and A-analyzer—illuminates a sample positioned between the poles of an electro-

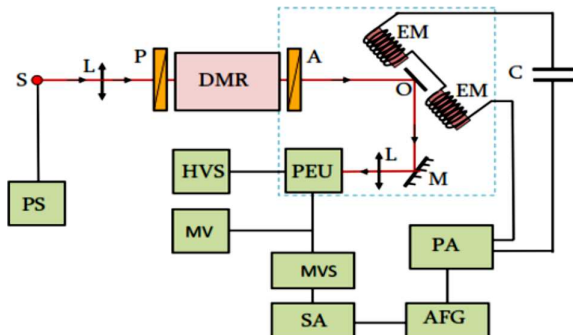


**Fig. 1.** Schematic diagram of the experimental setup used to measure magneto-optical reflection effects (S – light source; L – gathering lens; PS – bulb feeder source; DMR – monochromator; P – polarizer; A – analyzer; O – sample; EM – electromagnet; M – mirror; PEU – photo-receiver; SA – selective amplifier; HVS – high voltage rectifier; AFG – sound frequency generator; PA – amplifier; C – capacitor; MV – millivoltmeter; MVS – selective microvoltmeter)

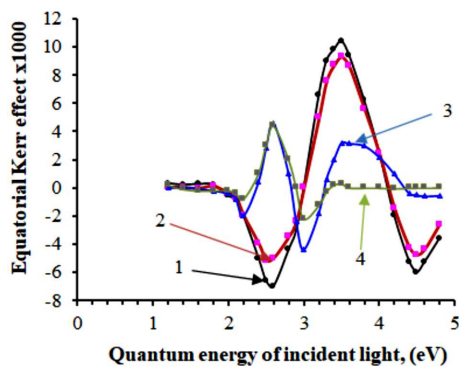


**Fig. 2.** Dependences of the equatorial Kerr effect on the quantum energy of incident light for the  $(\text{YBiCaSmLu})_3(\text{FeGeSi})_5\text{O}_{12}$  films before (curve 1) and after the process of implantation with doses:  $0.5 \times 10^{14}$  (curve 2),  $1.5 \times 10^{14}$  (curve 3), and  $2.5 \times 10^{14}$  (curve 4) ions/ $\text{cm}^2$ . The angle of the light incident on the sample is  $\varphi = 70^\circ$

magnet. The light reflected from the sample is focused on the photoreceiver through the M-mirror and L-light gathering lens. The electromagnet is powered by an alternating current with a frequency of 70–80 Hz, which is generated by the AFG frequency generator and amplified by the PA.

In our investigation of the magneto-optical behavior of ferrite-garnet surfaces, we focused on the linear magneto-optical reflection effects in two different Kerr configurations: polar and transverse. In the transverse Kerr effect, also known as the equatorial Kerr effect, magnetization  $\mathbf{M}$  is perpendicular to the plane

of incidence of light. In contrast, in the polar Kerr effect,  $\mathbf{M}$  is normal to the surface of the magnetic medium from which the optical wave is reflected.

These effects involve a change in the intensity of linearly polarized light reflected from the sample when the sample's magnetization is reversed. It can be expressed as follows:

$$\delta = \frac{I_H - I_{H=0}}{I_{H=0}} = \frac{U_{\sim}}{U_0}, \quad (1)$$

where  $I_H$  and  $I_{H=0}$  are, respectively, the intensities of light reflected from the magnetized and demagnetized samples, and  $U_{\sim}$  and  $U_0$  are the variable ( $U_{\sim}$ ) and constant ( $U_0$ ) components of the signal in the PEU (photo-receiver circuit).

The magneto-optical properties were measured at room temperature. The angle of the light incident on the sample was  $70^\circ$ .

### 3. Experimental Results and Discussion

We investigated the equatorial Kerr effect in the range of incident light quantum energies of 0.5–4.5 eV before and after ion-implantation of ferrite-garnet films for different compositions  $(\text{YBiCaSmLu})_3(\text{FeGeSi})_5\text{O}_{12}$ ,  $(\text{YBiCa})_3(\text{FeGe})_5\text{O}_{12}$ , and  $(\text{YBiCaSm})_3(\text{FeGeSi})_5\text{O}_{12}$ . Our experimental results are in close agreement with previously published works [10, 22]. For instance, Fig. 2 illustrates the relationship between the equatorial Kerr effect and the quantum energy of incident light for both unimplanted and ion-implanted  $(\text{YBiCaSmLu})_3(\text{FeGeSi})_5\text{O}_{12}$  films.

We observed magneto-optical maxima in the samples across all compositions at incident light quantum energy levels of 2.6, 3.5, and 4.5 eV (see Fig. 2).

It is important to note that the implantation process significantly affects the magneto-optical activity within these (2.6, 3.5, and 4.5 eV) energy ranges when the implantation doses exceed  $0.5 \times 10^{14}$  ions/ $\text{cm}^2$ . Additionally, it is worth emphasizing that for all compositions within the transparency range of ferrite-garnet thin films (0.5–2.2 eV), the magneto-optical effect is essentially negligible.

During the experiment, we observed that the deviation of the plane of polarization from the P-component of the incident light resulted in a significant magneto-optical effect within the energy range of 0.5 to 2.0 eV. In contrast, for incident light with quan-

tum energy ranging from 2.5 to 4.5 eV, the magneto-optical spectral characteristics of both unimplanted and implanted ferrite-garnet films remained practically unchanged.

For example, Figure 3 illustrates the relationship between the equatorial Kerr effect and the incident-light quantum energy for the  $(\text{YBiCaSmLu})_3(\text{FeGeSi})_5\text{O}_{12}$ ,  $(\text{YBiCa})_3(\text{FeGe})_5\text{O}_{12}$  films, both before and after the implantation process with a dose of  $2.0 \times 10^{14}$  ions/cm<sup>2</sup>. These measurements were taken at an angle of incidence of light on the sample ( $\varphi$ ) of  $70^\circ$  and a deviation angle of the polarization plane ( $\theta$ ) from the P-component of the incident light of  $5^\circ$ .

According to Fig. 3, the magneto-optical spectrum in the transparency range of both unimplanted and ion-implanted garnet surfaces shows a magneto-optical maximum at a light quantum energy of  $\hbar\omega = 1.4$  eV for  $(\text{YBiCa})_3(\text{FeGe})_5\text{O}_{12}$  (curves 1, 2) and  $\hbar\omega = 2.1$  eV for  $(\text{YBiCaSmLu})_3(\text{FeGeSi})_5\text{O}_{12}$  (curves 3, 4). It is important to emphasize that for all compositions, these magneto-optical maxima are observed within the transparency range of ferrite-garnet films (0.5–2.2 eV).

It is worth noting that the observed magneto-optical activity occurs under specific experimental conditions, particularly when the plane of polarization deviates from the P-component of the incident light. Typically, in the range of the specified incident quantum energy, the magnitude of the equatorial Kerr effect on the P-component of the polarization plane of the incident light is nearly zero (see Fig. 2).

Since the magneto-optical effects measured in the transparent region of ferrite-garnet films appear on the s-component of incident light, the intensity of the magneto-optical effects in the polar Kerr effect configuration has been measured on the same samples. In this setup, the magnetization vector is oriented perpendicular to the surface of the samples.

As an example, Figs. 4 and 5 illustrate dependences of the polar intensity magneto-optical effect (Fig. 4) and equatorial Kerr effect (Fig. 5) on the quantum energy of incident light  $\hbar\omega$  for the  $(\text{YBiCa})_3(\text{FeGe})_5\text{O}_{12}$  films before (curve 1) and after (curve 2) the implantation process with a dose of  $2.0 \times 10^{14}$  ions/cm<sup>2</sup>. The results of experimental research show that in both cases, the behavior of the spectral dependences of the magneto-optical effects in the range of  $\hbar\omega = 0.5$ –2.0 eV is the same.

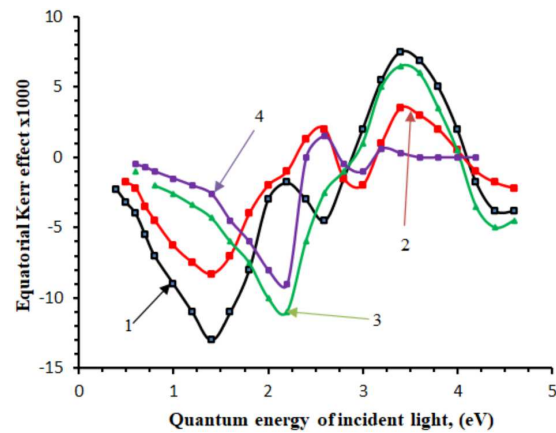


**Fig. 3.** Dependences of the equatorial Kerr effect on the quantum energy of incident light  $\hbar\omega$  for the  $(\text{YBiCa})_3(\text{FeGe})_5\text{O}_{12}$  (curves 1, 2) and  $(\text{YBiCaSmLu})_3(\text{FeGeSi})_5\text{O}_{12}$  (curves 3, 4) films before (curves 1, 3) and after the process of implantation with a dose  $2.0 \times 10^{14}$  ions/cm<sup>2</sup> (curves 2, 4), measured at  $\varphi = 70^\circ$ ,  $\theta = 5^\circ$

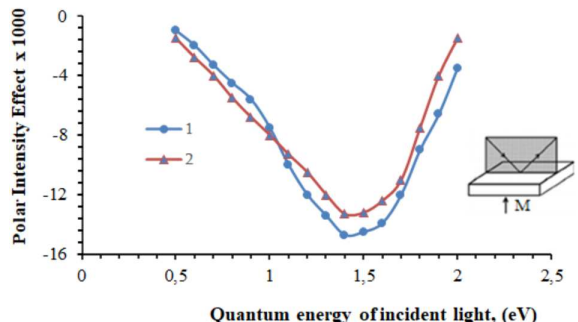


**Fig. 4.** Dependences of the polar intensity magneto-optical effect on the quantum energy of incident light for the  $(\text{YBiCa})_3(\text{FeGe})_5\text{O}_{12}$  films before (curve 1) and after (curve 2) the implantation process with a dose of  $2.0 \times 10^{14}$  ions/cm<sup>2</sup>, measured at  $\varphi = 70^\circ$ . The bottom right corner of the graph displays the configuration of the polar Kerr effect: vector of magnetization M is normal to the surface of the magnetic sample

The appearance of the equatorial Kerr effect in the energy range of 0.5 to 2.0 eV is attributed to the deviation of the polarization plane of the incident light ( $\theta$ ) from the P-component. Therefore, we examined how this magneto-optical activity depends on the angle  $\theta$ .

Fig. 6 shows the dependence of the equatorial Kerr effect on the angle of orientation of the polarization plane ( $\theta$ ), relative to the P component of the incident light for the  $(\text{YBiCaSmLu})_3(\text{FeGeSi})_5\text{O}_{12}$  before (curve 1) and after the process of implantation with

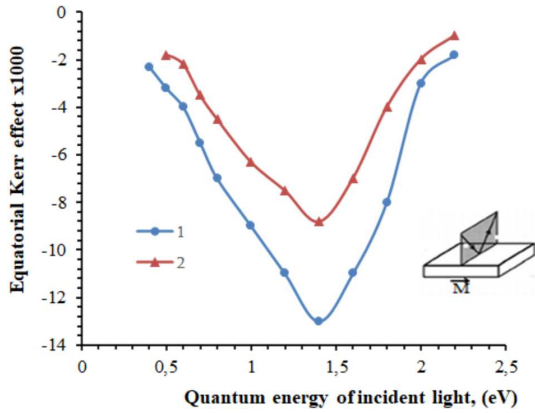


**Fig. 5.** Dependences of the equatorial Kerr effect on the quantum energy of incident light  $\hbar\omega$  for the  $(\text{YBiCa})_3(\text{FeGe})_5\text{O}_{12}$  films before (curve 1) and after (curve 2) the implantation process with a dose of  $2.0 \times 10^{14}$  ions/cm $^2$ , measured at  $\varphi = 70^\circ$ ,  $\theta = 5^\circ$  ( $\theta$  is the deviation angle of the polarization plane from the P-component of the incident light). The bottom right corner of the graph displays the configuration of the equatorial Kerr effect: vector of magnetization M is perpendicular to the plane of incidence of light

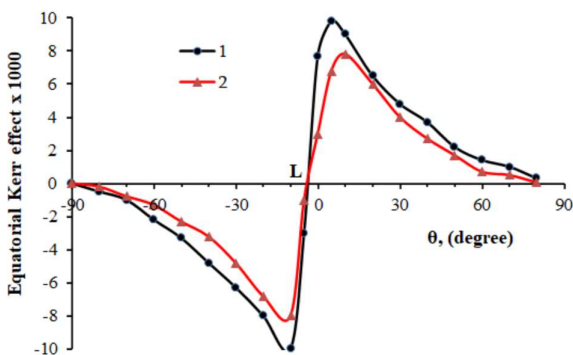


**Fig. 6.** Dependences of the equatorial Kerr effect on the angle  $\theta$  of orientation of the polarization plane from the P component of incident light for the  $(\text{YBiCaSmLu})_3(\text{FeGeSi})_5\text{O}_{12}$  before (curve 1) and after the process of implantation with a dose  $2.0 \times 10^{14}$  ions/cm $^2$  (curve 2) measured at  $\varphi = 70^\circ$  and  $\hbar\omega = 2.0$  eV

a dose  $2.0 \times 10^{14}$  ions/cm $^2$  (curve 2) measured at  $\varphi = 70^\circ$  and  $\hbar\omega = 2.0$  eV.

According to Fig. 6, the dependence of the equatorial Kerr effect on the angle ( $\theta$ ) is symmetric around point L, which is shifted by 2 to 3 degrees from the P component of the incident light. Similar dependencies of the magneto-optical effect on  $\theta$  have been reported in Ref. [22] for ferrite-garnet thin films of other compositions.

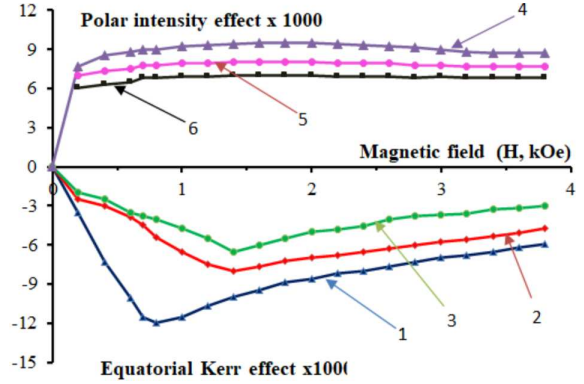


**Fig. 7.** Dependences of the equatorial Kerr effect on the magnitude of the external alternating magnetic field  $H_\sim$  for the  $(\text{YBiCa})_3(\text{FeGe})_5\text{O}_{12}$  (curve 1) at  $\hbar\omega = 1.6$  eV,  $(\text{YBiCaSm})_3(\text{FeGeSi})_5\text{O}_{12}$  (curve 2), and  $(\text{YBiCaSmLu})_3(\text{FeGeSi})_5\text{O}_{12}$  (curve 3) films at  $\hbar\omega = 2.0$  eV. The figure also presents similar dependences of polar intensity effect on  $H_\sim$  for the same films:  $(\text{YBiCa})_3(\text{FeGe})_5\text{O}_{12}$  (curve 4),  $(\text{YBiCaSm})_3(\text{FeGeSi})_5\text{O}_{12}$  (curve 5), and  $(\text{YBiCaSmLu})_3(\text{FeGeSi})_5\text{O}_{12}$  (curve 6). These measurements were taken after the implantation process with doses of  $2.0 \times 10^{14}$  ions/cm $^2$

We also measured the dependence shown in Fig. 6 in the polar configuration of the Kerr effect. In this case, the dependence of the polar intensity magneto-optical effect on  $\theta$  exhibited a similar behavior.

However, studies of the dependences of the magneto-optical Kerr effect on the value of the external magnetizing field in the range of  $\hbar\omega = 0.5$ – $2.0$  eV, in both equatorial and polar configurations, for ferrite-garnet films revealed that the nature of these dependences varies.

For instance, Fig. 7 illustrates dependences of the linear magneto-optical reflection effects on the magnitude of the external alternating magnetic field  $H_\sim$  in two different Kerr configurations: transverse (curves 1, 2, 3) and polar (curves 4, 5, 6) for the  $(\text{YBiCa})_3(\text{FeGe})_5\text{O}_{12}$  (curves 1, 4) at  $\hbar\omega = 1.6$  eV,  $(\text{YBiCaSm})_3(\text{FeGeSi})_5\text{O}_{12}$  (curves 2, 5), and  $(\text{YBiCaSmLu})_3(\text{FeGeSi})_5\text{O}_{12}$  (curves 3, 6) films at  $\hbar\omega = 2.0$  eV after the process of implantation with doses  $2.0 \times 10^{14}$  ions/cm $^2$  and at  $\theta = 5^\circ$ .

According to Fig. 7, curves 1, 2, and 3 exhibit a distinctive behavior. In weak magnetic fields, the equatorial Kerr effect increases up to a certain level. However, once the field strength slightly exceeds approximately (1.0–1.3) kOe, the magnitude of this effect begins to decrease. In contrast, the polar intensity effect

(represented by curves 3, 4, and 6) rapidly saturates at external demagnetizing field strengths of approximately 100 Oe.

To understand this complex behavior, we hypothesized that, at equatorial magnetization of garnet films with perpendicular anisotropy in the low magnetic field region ( $H_{\sim} < 1$  kOe), the presence of a small polar field component causes demagnetization of the sample along the easy magnetization axis, which is perpendicular to the sample's surface.

As the magnetic field strength increases ( $H_{\sim} > 1$  kOe), the equatorial Kerr effect decreases. This reduction can be attributed to the reorientation of the magnetization direction within the plane of the sample surface, leading to a diminished value of the Kerr effect.

A comprehensive study of the Kerr effect in the transparency region of ferrite-garnet films showed that both the magnitude and the sign of this effect depend significantly on the orientation of the magnetic field.

We have found that a slight deviation of the external alternating magnetic field from the plane of the sample causes a similar magneto-optical maximum to appear on the P-component of the incident light within the transparency region of garnet films. However, when the external magnetic field is aligned within the plane of the sample, the magneto-optical effect does not occur for the P-component of the incident light.

Therefore, the investigation of magnetization processes in the transparency region of garnet films indicates that the formation of magneto-optical effects is quite complex.

It is also important to highlight that the study of the magneto-optical properties of both implanted and non-implanted ferrite-garnet thin films has shown that in the region of incident light quantum energy from 0.5 to 2.2 eV, implantation virtually does not affect their magneto-optical properties.

#### 4. Conclusion

Magneto-optical reflection effects in the transparency region of ferrite-garnet thin films have been investigated. We have detected that a slight deviation of the plane of the external alternating magnetic field from the plane of the sample or a shift of the polarization plane away from the P-component of incident light leads to the appearance of an intensive magneto-

optical maximum in the transparency region of garnet films. As a result, the equatorial Kerr effect has been observed in the S-component of the incident light.

Experimental studies show that ion implantation has a significant impact on the magneto-optical properties of ferrite-garnet films when the incident-light quantum energy ranges from 2.5 to 4.5 eV. However, in the transparency range, specifically for energies of  $\hbar\omega = 0.5$  to 2.2 eV, the magneto-optical properties of these films virtually remain unchanged.

*This work was supported by Shota Rustaveli National Science Foundation of Georgia (SRNSFG) [grant number FR-24-3101]. Project title: Experimental and theoretical methods of magneto-optical research in spintronics.*

1. K. Ikeda, N. Kobayashi, K. Arai. Large Faraday effect in nanogrannular films with a high refractive index matrix. *Opt. Mater. Express.* **12**, 403 (2022).
2. Y. Nakamura, S.B. Chauhan, P.B. Lim. Magneto-optical properties and applications of magnetic garnet. *Photonics* **11** (10), 931 (2024).
3. Y. Yucong, L. Tao, Lei, D. Longjiang. Recent advances in development of magnetic garnet thin films for applications in spintronics and photonics. *J. Alloys and Compounds* **860**, 158235 (2021).
4. M. Nur-E-Alam, M. Vasilev, V. Belotelov, K. Alameh. Properties of ferrite garnet  $(\text{Bi}, \text{Lu}, \text{Y})_3(\text{Fe}, \text{Ga})_5\text{O}_{12}$  thin film materials prepared by RF magnetron sputtering. *Nanomaterials* **8** (5), 355 (2018).
5. H. Dötsch, N. Bahlmann, O. Zhiromskyy, M. Hammer, L. Wilkens, R. Gerhardt, P. Hertel, A. Popkov. Applications of magneto-optical waveguides in integrated optics: review. *J. Opt. Soc. Am. B* **22**, 240 (2005).
6. G. Vértesy. Coercive properties of magnetic garnet films. *Crystals* **13** (6), 946 (2023).
7. S. Oh, Y. Ko, D. Kang, K. Oh, S.H. Kim, K.H. Kyong Hon Kim. Optical and magneto-optical properties of bismuth-substituted neodymium iron gallium garnet films on glass substrates at the 1310-nm and 1550-nm wavelengths. *J. Magn. Magn. Mat.* **560**, 169606 (2022).
8. Y. Yang, T. Liu, L. Bi, L. Deng. Recent advances in development of magnetic garnet thin films for applications in spintronics and photonics. *J. Alloys Compd.* **860** 158235 (2021).
9. L. Dorosinskiy, S. Sievers. Magneto-optical indicator films: Fabrication, principles of operation, calibration, and applications. *Sensors* **23** (8), 4048 (2023).
10. L. Kalandadze. Influence of Implantation on the optical and magneto-optical properties of garnet surface. *J. Magn. Magn. Mat.* **373**, 160 (2015).
11. M. Saito, R. Tajima, R. Kiyosawa, Y. Nagata, Shimada, H.T. Ishibashi, A. Hatakeyama. Optical and magnetic

properties of a transparent garnet film for atomic physics experiments. *AIP Advances* **6**, 125023 (2016).

12. R. Jiang, X. Yang, J. Chen, S. Shen, S. Zhou, Y. Tian, J. Wang. Study on ion slicing of iron garnet magneto-optic materials for near and mid-infrared on-chip optical isolators. *Opt. Express* **32**, 49093 (2024).
13. I. Fodchuk, A. Kotsyubinsky, A. Velychkovych, I. Hutsuliak, V. Boychuk, V. Kotsyubinsky, L. Ropyak. The effect of  $Ne^+$  ion implantation on the crystal, magnetic, and domain structures of Yttrium Iron Garnet films. *Crystals* **12** (10), 1485 (2022).
14. L. Kalandadze. Influence of implantation on the magneto-optical properties of garnet surface. *J. IEEE Trans. on Magn.* **44**, (11), 3293 (2008).
15. T. Haider, A review of magneto-optic effects and its application. *Intern. J. Electromagnetics and Appl.* **7** (1), 17 (2017).
16. A. Kimel, A. Zvezdin, S. Sharma, S. Shallcross, N. Sousa, A. García-Martín, G. Salván, G. Hamrle, O. Stejskal, J. McCord. The 2022 magneto-optics roadmap. *Phys. D: Appl. Phys.* **55**, 463003 (2022).
17. S. Kumari. A comprehensive study of magneto-optic materials and its applications. *Mater. Today: Proc.* **56** (1), 100 (2022).
18. K. Srinivasan, B.J.H. Stadler. Magneto-optical materials and designs for integrated TE- and TM-mode planar waveguide isolators: A review [Invited]. *Opt. Mater. Express* **8**, 3307 (2018).
19. C. Rizal, H. Shimizu, J.R. Mejía-Salazar. Magneto-optics effects: New trends and future prospects for technological developments. *Magnetochemistry* **8** (9), 94 (2022).
20. L. Sheng, J. Chen, H. Wang, H. Yu. Magnonics based on thin-film iron garnets. *J. Phys. Soc. Jpn.* **90**, 081005 (2021).
21. D. Yan, H. Wang. Magneto-optical properties and gyration vectors of iron garnet films containing different bismuth ions. *Appl. Phys. A* **129**, 510 (2023).
22. L. Kalandadze. Investigation of the magneto-optical properties in transparent region of implanted  $(YBiCa)_3(FeGe)_5O_{12}$  garnet films. *IEEE 7th International Conference Nanomaterials: Application & Properties (NAP)*. 01PCSI11-1-01PCSI11-4 (2017).

Received 17.12.25

Л. Каландадзе, О. Накашідзе, Н. Гомідзе,  
М. Хаджішвілі, І. Джабабідзе, К. Махарадзе

### МАГНЕТООПТИЧНА ПОВЕДІНКА ІМПЛАНТОВАНИХ ТОНКИХ ФЕРИТ-ГРАНАТОВИХ ПЛІВОК У ДІАПАЗОНІ ПРОЗОРОСТІ

Тонкі ферит-гранатові плівки особливі магнетооптичні властивості, що робить їх дуже актуальними як для фундаментальних досліджень, так і для передових технологічних застосувань в оптиці, магнетизмі, електроніці, спінtronіці та фотоніці. З цієї точки зору особливого практичного значення набувають магнетооптичні властивості іонно-імплантованих ферит-гранатових плівок, оскільки іонна імплантація може зменшити або змінити локальну намагніченість, коерцитивну силу та анізотропію, а також послабити циліндричні магнетні домени, покращуючи можливості контролю та використання їхніх параметрів. У цій роботі ми досліджували магнетооптичний ефект Керра в діапазоні енергій квантів падаючого світла 0,5–4,5 еВ до та після іонної імплантації ферит-гранатових плівок різного складу  $(YBiCaSmLu)_3(FeGeSi)_5O_{12}$ ,  $(YBiCa)_3(FeGe)_5O_{12}$ , та  $(YBiCaSm)_3(FeGeSi)_5O_{12}$ . Було встановлено, що тонкі плівки ферит-гранатулюють цікаві магнетооптичні властивості в діапазоні енергій квантів падаючого світла 0,5–2,2 еВ. Зокрема, за певних експериментальних умов, спостерігається магнетооптична активність коли площа поляризації падаючого світла відхиляється від Р-компоненти. Для з'ясування природи цього ефекту було досліджено полярний ефект Керра та процеси намагнічування в діапазоні енергій квантів падаючого світла 0,5–2,2 еВ, що є областю прозорості ферит-граната. Отримані результати підтверджують, що в цій області магнетооптична активність характерна для всіх трьох досліджених зразків ферит-граната, а імплантація практично не впливає на їхні магнетооптичні властивості.

**Ключові слова:** тонкі плівки ферит-граната, м'які магнетні матеріали, іонна імплантація, магнетооптичні матеріали, магнетооптичні ефекти.